

Energy & Environmental Science

Accepted Manuscript



This is an *Accepted Manuscript*, which has been through the Royal Society of Chemistry peer review process and has been accepted for publication.

Accepted Manuscripts are published online shortly after acceptance, before technical editing, formatting and proof reading. Using this free service, authors can make their results available to the community, in citable form, before we publish the edited article. We will replace this *Accepted Manuscript* with the edited and formatted *Advance Article* as soon as it is available.

You can find more information about *Accepted Manuscripts* in the [Information for Authors](#).

Please note that technical editing may introduce minor changes to the text and/or graphics, which may alter content. The journal's standard [Terms & Conditions](#) and the [Ethical guidelines](#) still apply. In no event shall the Royal Society of Chemistry be held responsible for any errors or omissions in this *Accepted Manuscript* or any consequences arising from the use of any information it contains.

COMMUNICATION

Benefits of Very Thin PCBM and LiF Layer for Solution-Processed P-I-N Perovskite Solar Cells

Cite this: DOI: 10.1039/x0xx00000x

Jangwon Seo,^a Sangman Park,^a Young Chan Kim,^a Nam Joong Jeon,^a Jun Hong Noh,^a Sung Cheol Yoon^{*,a} and Sang Il Seok^{*,ab}

Received 00th April 2014,
Accepted 00th April 2014

DOI: 10.1039/x0xx00000x

www.rsc.org/

Highly efficient p-i-n perovskite solar cells employing a flat and thick $\text{CH}_3\text{NH}_3\text{PbI}_3$ film and a thin PCBM film are fabricated by solution-process at low temperature. Through the optimized PCBM thickness and insertion of LiF interlayer, unit cell shows 14.1% of overall power conversion efficiency (PCE) with a J_{sc} of 20.7 mA cm^{-2} , a V_{oc} of 0.866 V, and a FF of 78.3% under AM 1.5G 100 mW cm^{-2} condition, while larger area 10-cells serially connected module ($10 \times 10 \text{ cm}^2$) shows a 8.7% PCE. The PCEs are the highest value reported to date for the planar perovskite-PCBM solar cells.

Hybrid organic/inorganic perovskite materials with the formula $\text{CH}_3\text{NH}_3\text{PbI}_3$ (=MAPbI₃) have received a great deal of attention because of their good intrinsic properties for photovoltaic applications, such as an appropriate band gap (1.55 eV), high absorption coefficient, long hole-electron diffusion length (~100 nm), and excellent carrier transport.¹⁻¹³ Furthermore, these materials offer the chemical and structural diversity that can be obtained by mixing in various halides (Br or Cl) or replacing the methylammonium organic species with other constituents (ethylammonium, formamidium etc.).¹⁴⁻¹⁷ As a result, their band gaps, crystalline phase transitions, and hole-electron diffusion lengths can all be tuned. Recently, great progress has been made in perovskite solar cells employing an electron-transport layer/perovskite material/hole-transport layer structure, which facilitates selective hole extraction to the gold electrode.⁹⁻¹³ Although they exhibit high performance, the formation of most electron-transport layer such as mesoporous (mp)-TiO₂ layer requires high-temperature processing. Therefore, many approaches to avoiding high-temperature manufacturing (>450°C) for preparing a compact or mp-TiO₂ layer have been examined.^{18,19} As one promising approach, the use of phenyl-C61-butyric acid methyl ester (PCBM) in perovskite solar cells has been investigated by several groups.²⁰⁻²⁴ Furthermore, n-i-p architecture consisting of n-

TiO₂/perovskite/p-hole conductor suffers from a large hysteresis with the sweep direction in the measurement.^{25,26}

To fabricate p-i-n perovskite cells, ITO/poly(3,4-ethylenedioxythiophene):poly(styrenesulfonic acid) (PEDOT:PSS) substrate and PCBM is generally used. The perovskite layer, which acts as a light absorber, is deposited by spin-coating on top of the PEDOT:PSS layer, followed by a thin PCBM layer as the electron acceptor. Then, an Al electrode is usually used as the cathode electrode. Recent efforts to increase the device performance of PCBM/perovskite heterojunction solar cells have focused on establishing a thicker perovskite film (100–350 nm) to ensure better light absorption and a higher current density.²⁰⁻²⁴ Simultaneously, a well-controlled flat surface of the perovskite film is essential for deposition of a thin PCBM layer. Reducing the thickness of the PCBM layer leads to better photovoltaic device performance by increasing conductivity in the PCBM film.²⁷⁻²⁹ However, so far, there have been some obstacles to realizing a homogenous perovskite layer with a uniform thickness in a planar heterojunction cell by solution processing. To overcome the morphology problems associated with the roughness of the thick perovskite film, a thicker PCBM layer (>110 nm) can be used or another n-type layer (like TiO_x) can be deposited on the top of thin PCBM layer (~50 nm) to prevent leakage due to direct contact between the metal and the perovskite film.^{22,24}

Early 2014, Bolink and co-workers fabricated a planar heterojunction device with an efficiency as high as 12% under AM 1.5G 100 mW cm^{-2} irradiation using an evaporation method in a high-vacuum chamber.²³ This result demonstrates the great potential of the perovskite-PCBM architecture. However, it still remains a challenge to improve the performance of perovskite-PCBM heterojunction devices. Moreover, it is highly desirable to develop a low-cost solution-processable solar cell with a high efficiency, a large area, and

flexibility, especially one that can be fabricated at low temperatures.

Recently, we established a solvent-engineering technology employing a mixture solution of dimethyl sulfoxide (DMSO): γ -butyrolactone (GBL) (3:7, v/v) to create a highly uniform perovskite layer.²⁵ The presence of DMSO helps to retard the rapid reaction between the inorganic PbI_2 and $\text{CH}_3\text{NH}_3\text{I}$ components of perovskite by forming DMSO- PbI_2 complexes.³⁰ This allows a smoother film to be formed upon a consecutive spin-coating process.

In this work, we report the fabrication of a highly improved MAPbI_3 perovskite solar cell and the dependence of its device-performance on the thickness of PCBM layer. The optimized device with a 55-nm-thick PCBM layer and a LiF/Al cathode showed a high efficiency of 14.1% under AM 1.5G 100 mW cm^{-2} condition, which is the highest value reported to date for perovskite solar cells using normal OPV architectures fabricated using low-temperature processing. Furthermore, we demonstrate for the first time a solution-processing method for the fabrication of a larger area device ($10 \times 10 \text{ cm}^2$), which shows a power conversion efficiency (PCE) of 8.7%.

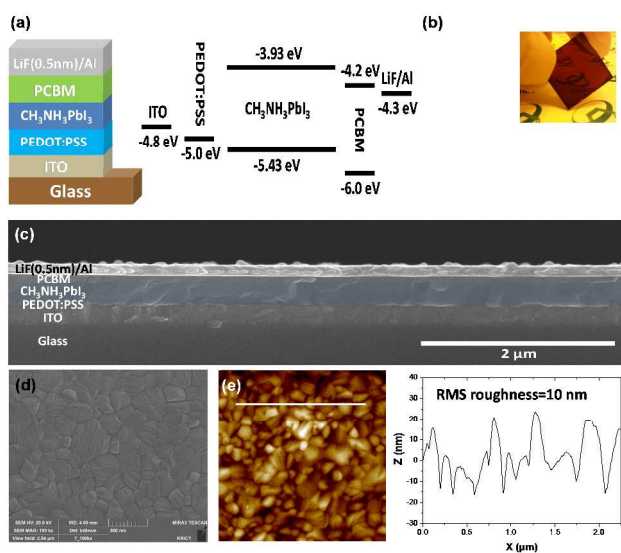


Fig. 1. (a) Device architecture of the ITO/PEDOT:PSS/ $\text{CH}_3\text{NH}_3\text{PbI}_3$ /PCBM/LiF/Al cells and energy levels of the various device layers. Here, energy levels for $\text{CH}_3\text{NH}_3\text{PbI}_3$ and PCBM were obtained from ref. 6 and 21, respectively. (b) UV-vis spectrum of a $\text{CH}_3\text{NH}_3\text{PbI}_3$ film on a quartz/PEDOT:PSS substrate prepared using solvent-engineering process. Inset shows a photograph of the film. (c) Cross-sectional SEM image showing the device structure of the $\text{CH}_3\text{NH}_3\text{PbI}_3$ /PCBM bilayer heterojunction solar cell. The thickness of PEDOT:PSS, $\text{CH}_3\text{NH}_3\text{PbI}_3$, and PCBM layers are 40, 290, and 120 nm, respectively. The perovskite layer is tinted with the different color. (d) SEM image of the top surface of the $\text{CH}_3\text{NH}_3\text{PbI}_3$ film on ITO/PEDOT:PSS surface. (e) Its AFM image and roughness profile.

Fig. 1a depicts the device configuration of the hybrid perovskite-PCBM heterojunction solar cell and the energy level diagram of each layer in the device. From the potential difference between the conduction band of MAPbI_3 perovskite as the donor and the lowest

unoccupied molecular orbital (LUMO) of the PCBM as the acceptor, we see that this configuration is suitable for efficient exciton dissociation and charge transport. Therefore, free charge carriers (or excitons) generated in the MAPbI_3 layer can be extracted (or dissociated) by electron transfer to the PCBM. The electrodes collect the photogenerated free carriers; the ITO collects holes and the cathode (Al metal) collects the electrons. As shown in Fig. 1b, the absorption spectrum is consistent with the typical spectrum of MAPbI_3 films over the entire UV and visible range up to 800 nm.⁷ A typical cross-sectional SEM image of the device is given in Fig. 1c. Our solvent-engineering technique can offer an extremely uniform and thick perovskite film ($\sim 290 \text{ nm}$) on the ITO/PEDOT:PSS substrate, even though the width is in the range of several tens of micrometers. Subsequently, PCBM layer is able to be deposited using orthogonal solvent processing. The well-crystallized perovskite covers the entire surface of the PEDOT:PSS layer perfectly. We also see that the fabricated film is dark brown in color, with good transparency (see the inset of Fig. 1b).

Fig. 1d displays the surface morphology of the fabricated MAPbI_3 film on top of the ITO/PEDOT:PSS layer. The film surface is composed of well-developed grains with sizes of a few hundred nanometers, and full surface coverage of PCBM is achieved. The homogenous and flat morphology is different from those of other films prepared by simple spin-coating.^{20,22,31} Atomic force microscopy (AFM) measurements showed that the 290-nm-thick film is very smooth with a rms (root mean square) roughness of about 10 nm in an area of $3 \mu\text{m} \times 3 \mu\text{m}$ (see Fig. 1e). Thus, the perovskite layer formed in this work has a very low roughness, which allows a thin ($< 100 \text{ nm}$ thick) PCBM layer.

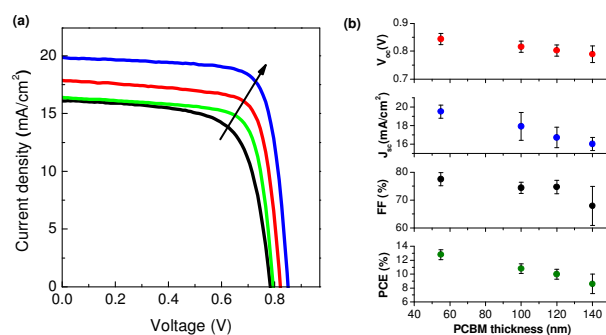


Fig. 2. (a) Average photocurrent density-voltage (J - V) characteristics of $\text{CH}_3\text{NH}_3\text{PbI}_3$ -PCBM heterojunction solar cells with PCBM layer thickness of 55, 100, 120, and 140 nm (blue, red, green, and black line, respectively), measured under simulated AM 1.5 100 mW cm^{-2} sunlight. (b) Dependence of the device performance on the corresponding thickness of the PCBM layer. Each data points represent the mean from a set of 11 or more devices.

To gain more insight into the effect of the thickness of the PCBM layer on the device performance, we fabricated hybrid solar cells with fixed thicknesses of MAPbI_3 layer but different thicknesses of the PCBM layer of 55, 100, 120, and 140 nm. The PCBM layer thickness was changed by varying the concentration of the PCBM spin-coating solution. Fig. S1 shows a top-view SEM image of the 55-nm-thick PCBM film deposited on ITO/PEDOT:PSS/ MAPbI_3 . It can be seen that the PCBM layer is

very smooth and covers the entire MAPbI₃ surface perfectly, even though it is only 55-nm-thick. From this result, it is reasonable to assume that the perovskite film can also be fully covered by PCBM layers thicker than 55 nm. Fig. 2a shows the photocurrent density-voltage (*J*-*V*) curves of MAPbI₃-PCBM heterojunction cells with different PCBM layer thickness. The details of the device parameters are given in Table S1. As the thickness of the PCBM layer decreases from 55 to 140 nm, the device efficiency greatly increases. (see Fig. 2b) A similar trend is observed for the short circuit current density (*J*_{sc}), open circuit voltage (*V*_{oc}), and fill factor (FF). For the 140-nm-thick PCBM layer in particular, the current density and the fill factor are quite low. This is probably due to increased recombination and a resultant high series resistance when the dissociated carriers travel longer distance to reach the Al electrode. The optimal device performance is obtained for the thin PCBM layer with a thickness of ~ 55 nm, which yield a PCE in excess of 12%. As compared to other MAPbI₃-PCBM heterojunction devices, this device also exhibited a substantial improvement in *J*_{sc}, reaching nearly 20 mA cm⁻². However, further decreases in the thickness of the PCBM layer deteriorated the device performance, greatly reducing *V*_{oc} and FF (see Fig. S2). This implies that leakage current may be occurred by the direct contact between perovskite layer and Al metal, when the PCBM layer becomes too thin (~40 nm). This observation can be explained by the roughness profile of the perovskite surface in Fig. 1e. If the direct contact between the Al metal and the perovskite layer occurs because of surface defects in the PCBM layer, the device performance can worsen because of the resulting leakage current. In addition, devices with thin PCBM layers (~40 nm) did not perform as reliably as the other devices with thicker PCBM layers. Accordingly, full surface coverage of the perovskite film by the PCBM layer is crucial to ensure the reproducibility of the device performance. Once this condition is met, a thinner PCBM layer is favorable for better device performance.

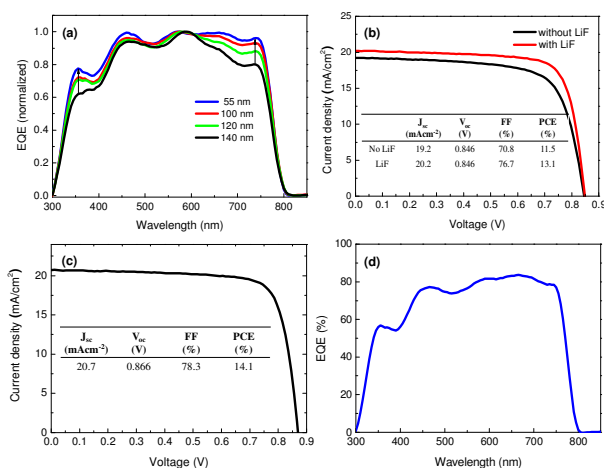


Fig. 3. (a) Normalized external quantum efficiency (EQE) spectra of CH₃NH₃PbI₃-PCBM heterojunction solar cells with PCBM layer thickness of 55, 100, 120, and 140 nm (green, blue, red, and black lines, respectively). (b) Photocurrent density-voltage (*J*-*V*) characteristics of the CH₃NH₃PbI₃-PCBM heterojunction solar cells without and with LiF (0.5 nm) layer. (c) Photocurrent density-voltage (*J*-*V*) characteristics of the champion device in

CH₃NH₃PbI₃-PCBM heterojunction solar cells with a PCBM layer thickness of 55 nm. (d) EQE spectrum of this device.

The external quantum efficiency (EQE) curves of devices with different thicknesses of the PCBM layer are shown in Fig. 3a. The spectra are normalized so that the amounts of charge collection in the absorption range can be compared. The shapes of the EQE in the range of 300 and 500 nm mainly originate from the transmittance spectrum of ITO/PEDOT:PSS,^{32,33} because the CH₃NH₃PbI₃ absorbs 100% of its incident radiation regardless of the thickness of the PCBM. Interestingly, the EQE at 350 nm decreases as the thickness of PCBM increases, which implies that the charge collection is inefficient for a thicker PCBM layer, since the same amount of charge carriers is generated from the same amount of absorption. Similar behavior is found in the range of 600–800 nm. Thus, the EQE spectra are affected by the PCBM thickness. However, because the absorbance of the perovskite film in the range of 600–800 nm is not 100% (see Fig. 1b), a thicker film would be necessary to harvest more red and near-infrared light, which would still affect the EQE spectra. In the real device, an enhancement of EQE in the range for thin PCBM-device might be probably caused by the additional absorption of light reflected from Al electrode at thin PCBM layer.

In this study, we introduced a thin LiF layer (~0.5 nm) as a buffer layer, prior to deposition of the Al electrode in our cell. This resulted in an simultaneous improvement in the FF and *J*_{sc}, relative to those of a device without LiF layer (see Fig. 3b). Such an effect of LiF insertion was already reported for organic solar cells, implying that the electron extraction from the PCBM to the LiF/Al is improved by the reduced energy barrier between them resulting from the generation of a dipole moment across the interfaces.^{34,35} By choosing the optimal thickness of the PCBM layer and inserting the LiF interlayer, we could fabricate efficient cells with PCE exceeding 14 % under AM 1.5G 100 mW cm⁻² irradiation with negligible hysteresis of the *J*-*V* curve for reverse and forward scan directions (see Fig. 3c and Fig. S3). 14.1% of PCE can be obtained with a *J*_{sc} of 20.7 mA cm⁻², a *V*_{oc} of 0.866 V, and a FF of 78.3%. To the best of our knowledge, the 14.1% PCE is the highest performance of a hybrid MAPbI₃-PCBM heterojunction solar cell to date. The integrated current density derived from the EQE spectra in Fig. 3d is in close agreement (within nearly 5%) with the value measured under simulated sunlight. In particular, our device exhibits a relatively high FF of 74%–78%, as compared with those of other previously reported devices based on the perovskite-PCBM heterojunction.²²⁻²⁴ Moreover, to test the stability of our devices, we stored an encapsulated device in ambient air in the dark. The encapsulated device showed good stability over one month and maintained 95% of its initial efficiency (see Fig. S4).

Based on this unit cell, we also fabricated a large area photovoltaic module as a first step toward practical photovoltaic application. A picture of the perovskite-PCBM module and the schematic of its structure are shown in Fig. 4a, b. In ITO-coated glass (10 × 10 cm²), ten single cells are interconnected in series with an overall active area of 60 cm². All the solution-processing steps are identical to those when the small area unit cell (with an active area of 0.09 cm²) was fabricated. As shown in Fig. 4c, the photovoltaic

module yields a PCE of 8.7% and 7.0% for 55 nm-thick and 120-nm-thick PCBM layers, respectively, which are the highest efficiencies reported to date, including those of mesoscopic perovskite-modules.³⁶ In this large-area module, the device with the thinner PCBM layer still showed better performance, as was the case of for the unit cell. The device parameters of the module with the 55-nm-thick PCBM layer are $J_{sc} = 1.9 \text{ mA cm}^{-2}$, $V_{oc} = 8.1 \text{ V}$, and $FF = 57\%$. These current and voltage characteristics of the series-type module with ten single cells are comparable to those (19.5 mA cm^{-2} and 0.84 V) of the small-area unit cell. However, the FF is much lower than that of the unit cell because of the higher series resistance, which is the main reason for the reduced PCE of the module.

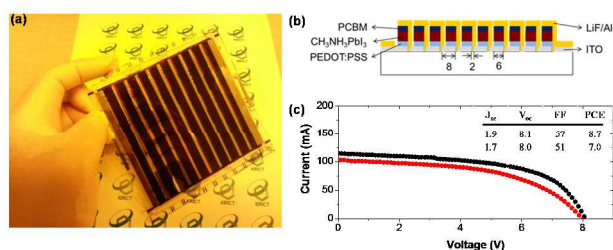


Fig 4. (a) Picture of the fabricated $\text{CH}_3\text{NH}_3\text{PbI}_3$ -PCBM heterojunction photovoltaic module (substrate size : $10\text{ cm} \times 10\text{ cm}$). (b) Schematic of the series-connected photovoltaic module. (c) Photocurrent density-voltage (J - V) characteristics of the photovoltaic module, measured under simulated AM 1.5 100 mW cm^{-2} sunlight where the thickness of PCBM layer is 55 nm and 120 nm (black and red line, respectively). The inset table shows the photovoltaic performance parameters, J_{sc} (mA/cm^2), V_{oc} (V), FF (%) and PCE (%).

Summary

In summary, we have demonstrated highly efficient p-i-n perovskite solar cells and $10 \times 10 \text{ cm}^2$ photovoltaic modules based on this unit cell. The deposition of a thin PCBM layer ($\sim 55 \text{ nm}$ thick) was made possible by the formation of extremely uniform perovskite layers, and the insertion of an LiF interlayer enabled the PCE to reach 14.1% for a unit cell and 8.7% for the module. These values are the highest reported to date for perovskite-PCBM planar heterojunction solar cells. Thus, this study provides new avenues for the fabrication of more efficient perovskite thin film solar cells using low-temperature solution processing and demonstrates the great potential of these technologies for achieving a large-area flexible photovoltaic device.

Acknowledgements

This research was supported by the Global Research Laboratory (GRL) Program, the Global Frontier R&D Program of the Center for Multiscale Energy System funded by the National Research Foundation in Korea, and by a grant from the KRICT 2020 Program for Future Technology of the Korea Research Institute of Chemical Technology (KRICT), Republic of Korea.

Notes and references

^a Division of Advanced Materials, Korea Research Institute of Chemical Technology, 141 Gajeong-Ro, Yuseong-Gu, Daejeon 305-600, Republic of Korea.

^b Department of Energy Science, Sungkyunkwan University, Suwon 440-746, Republic of Korea.

† Electronic Supplementary Information (ESI) available: A description on detailed experimental process, and characterization. See DOI: 10.1039/c000000x/

* To whom correspondence should be addressed. E-mail: seoksi@kriict.re.kr (seoksi@skku.edu) and yoonsch@kriict.re.kr

1. K. Liang, D. B. Mitzi and M. T. Prikas, *Chem. Mater.* 1998, **10**, 403-411.
2. A. Kojima, K. Teshima, Y. Shirai and T. Miyasaka, *J. Am. Chem. Soc.* 2009, **131**, 6050-6051.
3. J.-H. Im, C. R. Lee, J. W. Lee, S. W. Park and N. G. Park, *Nanoscale* 2011, **3**, 4088-4093.
4. L. Etgar, P. Gao, Z. S. Xue, Q. Peng, A. K. Chandiran, B. Liu, M. K. Nazeeruddin and M. Grätzel, *J. Am. Chem. Soc.* 2012, **134**, 17396-17399.
5. M. M. Lee, J. Teuscher, T. Miyasaka, T. N. Murakami and H. J. Snaith, *Science* 2012, **338**, 643-647.
6. H.-S. Kim, C.-R. Lee, J.-H. Im, K.-B. Lee, T. Moehl, A. Marchioro, S.-J. Moon, R. Humphry-Baker, J.-H. Yum, J. E. Moser, M. Grätzel, and N.-G. Park, *Sci. Rep.* 2012, **2**, 1-7.
7. J. H. Noh, S. H. Im, J. H. Heo, T. N. Mandal and S. I. Seok, *Nano Lett.*, 2013, **13**, 1764-1769.
8. J. H. Heo, S. H. Im, J. H. Noh, T. N. Mandal, C.-S. Lim, J. A. Chang, Y. H. Lee, H. Kim, A. Sarkar, M. K. Nazeeruddin, M. Grätzel and S. I. Seok, *Nat. Photon.* 2013, **7**, 486-491.
9. J. Burschka, N. Pellet, S.-J. Moon, R. Humphry-Baker, P. Gao, M. K. Nazeeruddin and M. Grätzel, *Nature*, 2013, **499**, 316-319.
10. M. Liu, M. B. Johnston and H. J. Snaith, *Nature*, 2013, **501**, 395-398.
11. H. J. Snaith, *J. Phys. Chem. Lett.* 2013, **4**, 3623-3630.
12. M. D. McGehee, *Nature* 2013, **501**, 323-325.
13. S. Kazim, M. K. Nazeeruddin, M. Grätzel and S. Ahmad, *Angew. Chem. Int. Ed.* 2014, **53**, 2-15.
14. G. C. Xing, N. Mathews, S. Sun, S. S. Lim, Y. M. Lam, M. Grätzel, S. Mhaisalkar and T. C. Sum, *Science*, 2013, **342**, 344-347.
15. S. D. Stranks, G. E. Eperon, G. Grancini, C. Menelaou, M. J. P. Alcocer, T. Leijtens, L. M. Herz, A. Petrozza and H. J. Snaith, *Science*, 2013, **342**, 341-344.
16. T. M. Koh, K. Fu, Y. Fang, S. Chen, T. C. Sum, N. Mathews, S. G. Mhaisalkar, P. P. Bois and T. Baikie, *J. Phys. Chem. C* 2014, DOI: 10.1021/jp411112k.
17. G. E. Eperon, S. D. Stranks, C. Menelaou, M. B. Johnston, L. M. Herz and H. J. Snaith, *Energy Environ. Sci.* 2014, **7**, 982-988.
18. J. T. Wang, J. M. Ball, E. M. Barea, A. Abate, J. A. Alexander-Webber, J. Huang, M. Saliba, I. Mora-Sero, J. Bisquert, H. J. Snaith, *et. al. Nano Lett.* 2014, **14**, 724-730.
19. D. Liu and T. L. Kelly, *Nat. Photonics* 2014, **8**, 133-138.
20. J. Y. Jeng, Y. F. Chiang, M. H. Lee, S. R. Peng, T. F. Guo, P. Chen and T. C. Wen, *Adv. Mater.* 2013, **25**, 3727-3732.
21. S. Y. Sun, T. Salim, N. Mathews, M. Duchamp, C. Boothroyd, G. Xing, T. C. Sum and Y. M. Lam, *Energy Environ. Sci.* 2014, **7**, 399-407.

22. P. Docampo, J. M. Ball, M. Darwich, G. E. Eperon and H. J. Snaith, *Nat. Commun.* 4:2761 DOI: 10.1038/ncomms3761.
23. O. Malinkiewicz, A. Yella, Y. H. Lee, G. M. Espallargas, M. Graetzel, M. K. Nazeeruddin and H. J. Bolink, *Nat. Photonics* 2014, **8**, 133-138.
24. J. You, Z. Hong, Y. M. Yang, Q. Chen, M. Cai, T.-B. Song, C.-C. Chen, S. Lu, Y. Liu, H. Zhou and Y. Yang, *ACS Nano* 2014, **8**, 1674-1680.
25. N. J. Jeon, J. H. Noh, Y. C. Kim, W. S. Yang, S. Ryu and S. I. Seok, *Submitted*.
26. H. J. Snaith, A. Abate, J. M. Ball, G. E. Eperon, T. Leijtens, N. K. Noel, S. D. Stranks, J. T.-W. Wang, K. Wojciechowski, and W. Zhang, *J. Phys. Chem. Lett.* 2014, **5**, 1511-1515
27. L. Dou, J. You, Z. Hong, Z. Xu, G. Li, R. A. Street and Y. Yang, *Adv. Mater.* 2013, **25**, 6642-6671.
28. N. R. Armstrong, W. Wang, D. M. Alloway, D. Placencia, E. Ratcliff and M. Brumbach, *Macromol. Rapid Commun.* 2009, **30**, 717-731.
29. A. L. Ayzner, C. J. Tassone, S. H. Tolbert and B. J. Schwartz, *J. Phys. Chem. C.* 2009, **113**, 20050-20060.
30. H. Miyamae, Y. Numahata and M. Nagata, *Chem. Lett.* 1980, 663-664.
31. G. E. Eperon, V. M. Burlakov, P. Docampo, Alain. Goriely and H. J. Snaith, *Adv. Func. Mater.* 2014, **24**, 151-157.
32. Z. Tan, W. Zhang, D. Qian, C. Cui, Q. Xu, L. Li, S. Li and Y. Li, *Phys. Chem. Phys. Chem.* 2012, **14**, 14217-14223.
33. Y.-F. Chiang, J.-Y. Jeng, M.-H. Lee, S.-R. Peng, P. Chen, T.-F. Guo, T.-C. Wen, Y.-J. Hsu and C.-M. Hsu, *Phys. Chem. Phys. Chem.* 2014, **16**, 6033-6040.
34. K.-S. Liao, S. D. Yambem, A. Haldar, N. J. Alley and S. A. Curran, *Energies* 2010, **3**, 1212-1250.
35. C. J. Brabec, S. E. Shaheen, C. Winder, N. S. Sariciftci and P. Denk, *Appl. Phys. Letts.* 2002, **80**, 1288-1290.
36. F. Matteocci, S. Razza, F. D. Giacomo, S. Casaluci, G. Mincuzzi, T. M. Brown, A. D'Epifanio, S. Licocchia and A. D. Carlo, *Phys. Chem. Chem. Phys.* 2014, **16**, 3918-3923.

TOC

Optimal thickness of PCBM layer and inserting the LiF interlayer on a well-controlled flat surface of the perovskite film is essential for fabricating planar perovskite-PCBM solar cells.

